

Collisions between two dissipative optical bullets separated in space

Ya Li (李 亚), Long Luo (罗 龙), and Yi Tang (唐 翌)*

Department of Physics and Institute of Modern Physics, Xiangtan University, Xiangtan 411105, China

*Corresponding author: tangyii@yahoo.cn

Received February 23, 2011; accepted April 21, 2011; posted online July 11, 2011

We present the numerical results of both head-on and non-head-on collisions between two stable dissipative optical bullets (DOBs) in a three-dimensional complex Ginzburg-Landau equation with cubic-quintic nonlinearity. The system parameters chosen are in the coexistence regions for both stationary DOBs and double bullet complexes (DBC). By varying the initial velocities v and the impact parameters P which represent the distance between the parallel trajectories of colliding bullets, we observe three generic properties of the bullets: fusion, fission, and quasi-elastic collisions. A novel and interesting behavior is observed in the results, in which two or three DBCs occur in non-head-on collisions at intermediate values of v .

OCIS codes: 060.5530, 190.5530, 320.7110.

doi: 10.3788/COL201109.100602.

Recently, the concept of the dissipative soliton, which is rooted in the classical soliton theory, the nonlinear dynamics theory of bifurcations, and the concept of self-organization proposed by Prigogine, has received increased attention^[1]. Dissipative solitons are recognized as fixed localized solutions resulting from a double balance: between dispersion and nonlinearity on one hand and between gain and loss on the other hand. Taking fiber laser as an example, the high-order vector soliton^[2] and the dissipative dark soliton^[3] occur as the balance between laser gain saturation and output loss, and the balance between cavity dispersion and the fiber nonlinear Kerr effect. Further, all dissipative solitons can only survive in the presence of a continuous energy supply. The cubic quintic complex Ginzburg-Landau equation (CGLE) is one of the notable models to describe dissipative solitons and is also applied to describe a variety of phenomena in optics. For example, CGLE appears in resonant atomic systems under electromagnetically induced transparency^[4] and gain-assisted systems^[5,6].

The dissipative optical system described by CGLE receives solitons in one-, two-, and three-dimensional (1D, 2D, and 3D)^[7]. The formed solitons can propagate stably, provided that the system parameters are carefully chosen in the specified regions. 1D and 2D dissipative solitons have been studied extensively^[4,8], but the solitons in 3D systems have not. The spatial-temporal soliton in 3D dissipative optical systems, usually called dissipative optical bullet (DOB), is created by the combined interplay of physical effects such as gain and loss, spectral filtering and dispersion, and diffraction and nonlinearity. Similar to what atoms are combined together to form a diatomic molecule, DOBs can be bound into the bullet molecule as well. The bullet molecule, called double bullet complex (DBC), appears as a localized structure that can be stationary, pulsating, and rotating. Meanwhile, DOBs can coexist with DBCs in nonlinear dissipative systems, which form some parameter regions of coexistence. The bistability in these regions can be applied to switch to the desired state using an applied control beam^[9] which offers a well-controlled platform for future investigations.

The interactions between DOBs are of fundamental importance to wide applications in all-optical logic and switching devices. A number of studies have been devoted to this subject. Using spherically symmetric CGLE, Rosanov was the first to examine the interactions between optical bullets in an anomalous dispersive medium^[7]. Mihalache *et al.* investigated the collisions between spatiotemporal dissipative vortex solitons^[10]. Soto-Crespo *et al.* showed that optical light bullets could coexist with DBCs in nonlinear dissipative systems^[9]. However, to the best of our knowledge, the dynamical features of the collision between two DOBs separated in space have not been studied well to date, especially in the coexistence system parameter regions of DOB and DBC. Therefore, in this letter, we present the numerical results for both head-on and non-head-on collisions between two DOBs with different velocities in the coexistence region. The observations from these simulations include fusion of the bullets into a rotating DBC, fission into two or three bullets, and quasi-elastic collision. A novel, interesting behavior is observed from the results: two or three DBCs are generated at intermediate values of velocities by carefully choosing the initial condition.

Our simulations are based on an extended CGLE model whose normalized propagation equation is^[9]

$$i \frac{\partial U}{\partial z} + \frac{D}{2} \frac{\partial^2 U}{\partial t^2} + \frac{1}{2} \frac{\partial^2 U}{\partial x^2} + \frac{1}{2} \frac{\partial^2 U}{\partial y^2} + |U|^2 U + \kappa |U|^4 U \\ = i\delta U + i\varepsilon |U|^2 U + i\beta \frac{\partial^2 U}{\partial t^2} + i\mu |U|^4 U. \quad (1)$$

The equation is written in “optical” notation, assuming evolution along the propagation coordinate z of a beam with the 3D cross section in the plane. In this case, $U(t, x, y, z)$ is the local amplitude of the normalized envelope of the field, D is the group velocity dispersion coefficient, δ represents the linear loss (if negative), ε is the nonlinear gain coefficient (if positive), β is the spectral filtering^[11], μ characterizes the saturation of the nonlinear gain (if negative), and κ is the parameter of quintic nonlinearity^[12]. System parameters are chosen in the right region where DOB and DBC can co-

exist: $D = 1$, $\mu = -0.1$, $\kappa = -0.1$, $\delta = -0.4$, $\varepsilon = 0.66$, and $\beta = 0.1$. Equation (1) is solved by the 3D split-step Fourier method. Therefore, periodic boundary conditions are used in x , y , and t . Most of the simulations presented are carried out on a $256 \times 256 \times 256$ mesh. For each case, the initial configuration to simulate a stationary bullet is produced by a preliminary step. We use an initial configuration in the following form:

$$U(t, x, y, z) = 3.0 \exp \left[- \left(\frac{x}{1.2} \right)^2 - \left(\frac{y}{1.2} \right)^2 - \left(\frac{z}{1.2} \right)^2 \right]. \quad (2)$$

Given the initial radial symmetry of the solution, the numerical integration of Eq. (1) can lead to a quick self-trapping of the input pulse into a stable stationary localized solution. One of the major characteristics of the DOB and DBC is the total amount of energy Q , which is defined by

$$Q(z) = \int_{-\infty}^{\infty} \int_{-\infty}^{\infty} \int_{-\infty}^{\infty} |U(x, y, z, t)|^2 dx dy dt. \quad (3)$$

If the solution remains localized, the energy evolves but remains finite. When a stationary DOB or DBC is reached, the total energy Q converges to a constant value.

The collision in the 3D system is complicated because the results depend on the equation parameters and the initial conditions. Each of the DOBs is stable, but the initial velocity and the impact parameter are still needed to describe the collision angle and the initial positions of the bullets. Therefore, to model a collision of the two stable DOBs moving at a finite angle toward each other, we use the following initial condition:

$$U(t, x, y, z = 0) = U_0 \left(t, x + \frac{R}{2}, y + \frac{P}{2} \right) \exp(ivx) + U_0 \left(t, x - \frac{R}{2}, y - \frac{P}{2} \right) \exp(-ivx), \quad (4)$$

where U_0 is the stable stationary localized solution of Eq. (1), and R stands for the initial separation between two bullets (we set $R = 16$ in our simulation), and P represents the impact parameter which is the distance between the parallel trajectories of the colliding solitons. Notably, the non-zero impact parameter can provide an initial angular momentum which is an adequate condition for the formation of a rotating DBC. The initial velocity v , which represents the amount of spatial chirp, is related to the angle of collision^[13]. The collision angle plays an important role in the collision problem in a variety of non-integrable systems^[14,15]. According to the waveguide theory of Snyder *et al.*^[16], a soliton can be viewed as a guided mode of its own self-induced waveguide^[17]. θ_c is the (complementary) critical angle for the total internal reflection in the waveguide. When they collide at $\theta > \theta_c$, solitons go through each other unaffected^[18,19], whereas for $\theta < \theta_c$, solitons can couple light into each other's waveguides. Therefore, the collisions are inelastic, leading to fusion or fission^[20]. Our results correspond with the qualitative theory above.

A diagram summarizing the outcomes of the collisions is shown in Fig. 1. Corresponding to each result, we illustrated our observation using the contour plots of $|U(t = 0, x, y = 0, z)|$ in Figs. 2 and 3. The collisions with a nonzero impact parameter cannot be properly studied

in the xz plane, so we select a set of snapshots of the distribution of $|U(t = 0, x, y, z = z_0)|$ which are depicted in Figs. 4 and 5. First, two cases of soliton fusion are given in Fig. 2. For head-on collisions in Fig. 2(a), the two DOBs initially move in opposite directions, and then they collide in the center of the mesh and merge into a single pulse. However, the simulations also show that the formed structure is unstable and pulsates in the spatial dimension over a relatively large interval of propagation distance (from $z = 10$ to 420). Finally, this instability destroys the bullets' radial symmetry and triggers the formation of a DBC with an energy around 184, which is more than twice the energy (around 68) of a single bullet. The regular serrated graphics with a width of about 9.2 in the contour plots of $|U(t = 0, x, y = 0, z)|$ indicates the formation of a DBC. Note that a detailed description of the transition from a pulsating bullet to a rotating DBC is also presented^[21]. Non-head-on collisions can also result in soliton fusion, and a typical example is given in Fig. 2(b). The initial condition here is the same as that in the previous case except that the impact parameter P is set to 0.5. However, compared with the head-on cases,

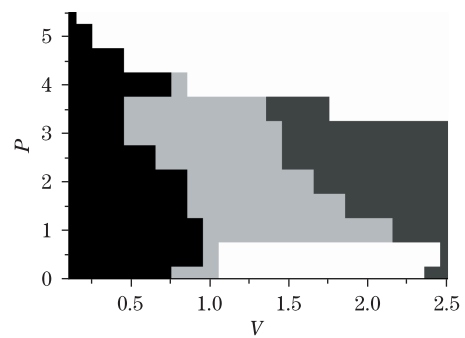


Fig. 1. Outcomes of collisions between two DOBs moving at velocities $\pm v$ with impact parameters P . The black, light gray, white, and dark gray colors mark the parameter regions where the fusion into two, fission into three, and quasi-elastic collision have been observed. The upper boundary of the diagram marks the critical value of the impact parameter for different velocities.

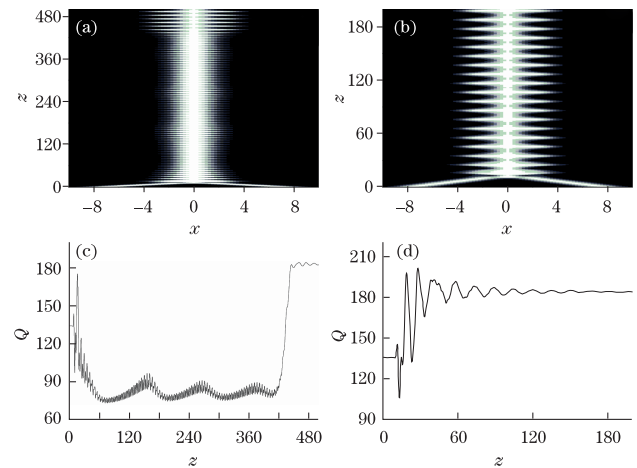


Fig. 2. Contour plot of $|U(t = 0, x, y = 0, z)|$ displaying the fusion of two DOBs into a DBC for the same initial velocities but different impact parameters: (a) $R = 16$, $P = 0$, $v = 0.6$; (b) $R = 16$, $P = 1.0$, $v = 0.6$; (c) and (d) show the total energy Q versus their propagation z corresponding to the cases in (a) and (b).

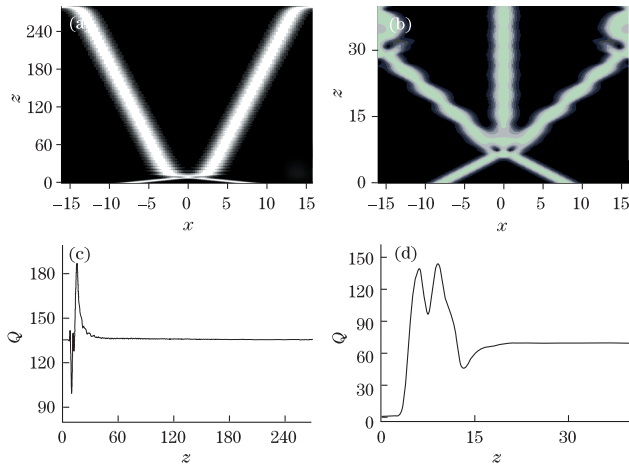


Fig. 3. Contour plot of $|U(t = 0, x, y = 0, z)|$ displaying the fission of two colliding DOBs into two or three bullets for both head-on collisions but at different velocities: (a) $R = 16$, $P = 0$, $v = 0.8$; (b) $R = 16$, $P = 0$, $v = 1.1$. (c) and (d) Show the total energy and the energy of the quiescent bullet corresponding to the cases in (a) and (b).

short propagation distances are needed to form a DBC. This is due to the nonzero impact parameter that gives an initial angular momentum which serves as a seed for the rotation at least at the birth of the rotating DBC. After the complex is formed, it rotates with a constant angular velocity space and possesses long-term stability with constant energy.

Second, with the increase in initial velocity, solution fission according to the scheme $1+1 \rightarrow 1+1$ is observed. One example of head-on collision is shown in Fig. 3(a): two bullets merge into a single pulse at first, but the pulse fails to self-trap into a single DOB or a DBC. Instead, it gives rise to fission into two optical bullets after short-term oscillation. Their energy suffers from slight perturbation, but it can be restored immediately to the initial value as shown in Fig. 3(c). In addition to energy oscillation, the velocities of the two pulsating bullets decrease due to inelastic collisions. Moreover, running the simulations in the domain with periodic boundary conditions, the two bullets collide with a smaller collision angle in the boundary and merge into one bullet which spontaneously transforms into a DBC as the case shown in Fig. 2(a). For the non-head-on case as shown in Fig. 4, however, the formation of the first fusion demonstrates an interesting dynamic behavior including rotation and elongation of spatial intensity profile. After fission into two bullets, each one gets an initial angular momentum, and the value of the offset between their trajectories in the vertical direction increases after the collision. The fission also causes some redistribution of energy, which affects the spatial shape of each bullet after collision. When the two bullets arrive at the boundary of the mesh simultaneously, the value of the offset is greater than the critical value. Without subsequent collision, the bullets moving in the mesh with the same velocity evolve into two rotating DBCs at $z \approx 100$. Their rotation has the same fixed angular velocity and rotates in the same direction (counterclockwise), which is determined by the initial conditions.

Third, in the narrow region marked white in Fig. 1, the generation of an extra bullet is observed according

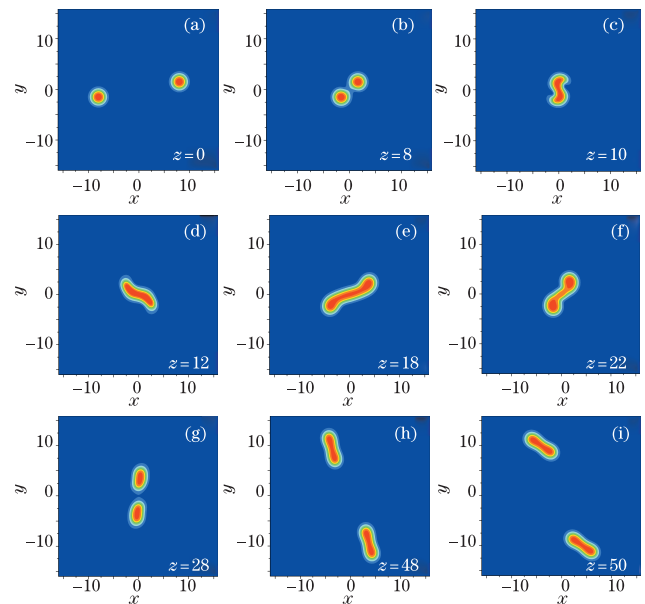


Fig. 4. Set of snapshots of the distribution of $|U(t = 0, x, y, z = z_0)|$ in the xy plane displaying the fission of the colliding bullets into two DBCs. $R = 16$, $v = 0.8$, and $P = 3.0$.

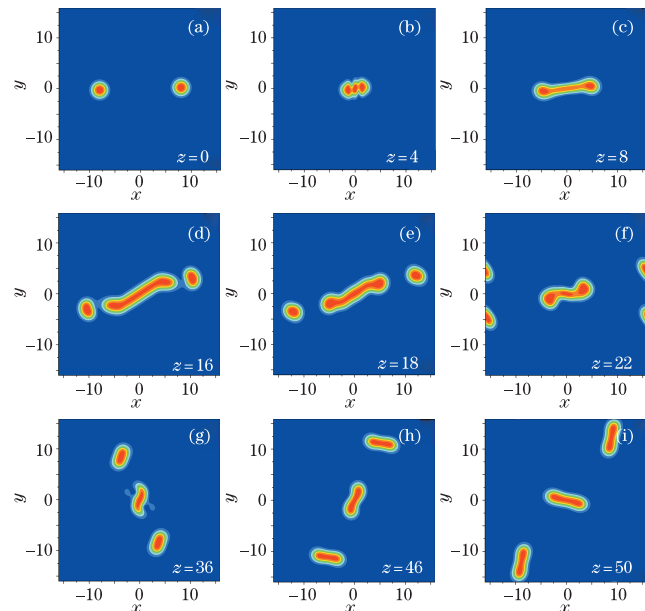


Fig. 5. Set of snapshots of the distribution of $|U(t = 0, x, y, z = z_0)|$ in the xy plane displaying the generation of three DBCs. $R = 16$, $v = 1.7$, and $P = 0.50$.

to the scheme $1+1 \rightarrow 1+1+1$. For both head-on and non-head-on collisions, we obtain one bullet with no velocity in the center of the mesh and two moving bullets whose dynamic behavior is similar to the scheme $1+1 \rightarrow 1+1$. The initial shape of a bullet is relevant but plays a secondary role if only one type of optical bullet exists for a given set of parameters. The shape becomes highly important when several stable solutions coexist^[9]. For the initial shape and energy of the newly created bullet which increase with an increase in collision velocity, we can obtain a single DOB around $v = 1.1$ but a DBC in a bigger velocity. The generation of a single DOB for head-on collision is shown in Fig. 3(b). The quiescent

bullet turned to be a single DOB which possesses long-term stability with constant energy after a finite number of oscillations. Meanwhile, the energy of the quiescent bullet may be obtained by counting only the energy Q of the interval of $[-3, +3]$ in the x axis, as shown in Fig. 3(d). When the initial velocity increases, the newly created bullet's radial symmetry is broken and converges after a long process to a rotating DBC. For the non-head-on collisions, Fig. 5 gives an example of the generation of three DBCs. Two incident bullets initially merge into one pulse whose spatial intensity profile remains elongated in the space domain until the system can no longer hold it, resulting in fission into three rotating bullets. The central bullet has a higher energy and broader profile than the DBC at the chosen set of parameters. Therefore, its spatial profile shrinks rapidly accompanied with a decrease in energy until the formation of a DBC. Another two moving bullets keep the central symmetry in the mesh and finally evolve into two DBCs if we choose the initial condition carefully. The rotation direction of the newly created bullet is different from that of the two moving bullets. Notably, the transformation of two colliding solitons into three (one quiescent and two moving) has also been experimentally observed and numerically demonstrated in many Hamiltonian and dissipative systems^[20,22,23].

Finally, by colliding two DOBs with large velocities, we observe the straightforward quasi-elastic passage of the bullets through each other for both head-on or non-head-on collisions. Moreover, given the periodic boundary conditions, multiple quasi-elastic collisions can also be observed by carefully choosing the initial condition. Compared with the inelastic collisions shown in Fig. 3(a), there are two differences: the velocities of the two bullets are almost unaffected after the collision compared with their original velocities. Their energy suffers from a slight perturbation but finally reaches a stable state, in which the energy of the bullets slightly fluctuates in a simple periodic form, agreeing with Refs. [24,25]. The disturbance caused by the soliton collision may lead to soliton collapse. However, the bullets in the initial condition in the current paper have a large shape and energy which can withstand the disturbance caused by the soliton collision at big velocities.

In conclusion, based on the 3D CGLE equation, we perform direct numerical simulations and examine systematically the collisions between two DOBs separated in space. This model can be applied to model a wide-aperture laser cavity in the short pulse regime of operation. By varying the initial velocities and the impact parameters, we observe three generic properties of bullets and the generation of two or three DBCs occurring in non-head-on collisions at intermediate values of v . Our results may be useful to other solitons such as those in active-Raman-gain medium^[26] and radially periodic optical lattices^[27]. The findings can also be applied to information transmission, all-optical logic, switching devices, and so on.

This work was supported by the Key Project of Hunan Provincial Educational Department of China under Grant No. 04A058.

References

1. N. Akhmediev and A. Ankiewicz, *Dissipative Solitons: From Optics to Biology and Medicine* (Springer, Heidelberg, 2008).
2. D. Y. Tang, H. Zhang, L. M. Zhao, and X. Wi, Phys. Rev. Lett. **101**, 153904 (2008).
3. H. Zhang, D. Y. Tang, L. M. Zhao, and X. Wu, Phys. Rev. A **80**, 045803 (2009).
4. C. Hang, G. Huang, and L. Deng, Phys. Rev. E **73**, 036607 (2006).
5. C. Zhu and G. X. Huang, Opt. Express **19**, 1963 (2011).
6. H. Li, L. Dong, C. Hang, and G. Huang, Phys. Rev. A **83**, 023816 (2011).
7. N. N. Rosanov, *Spatial Hysteresis and Optical Patterns* (Springer, Berlin, 2002).
8. L.-C. Crasovan, B. A. Malomed, and D. Mihalache, Phys. Lett. A **289**, 59 (2001).
9. J. M. Soto-Crespo, N. Akhmediev, and Ph. Grelu, Phys. Rev. E **74**, 046612 (2006).
10. D. Mihalache and D. Mazilu, Rom. Rep. Phys. **61**, 175 (2009).
11. G. P. Agrawal, Phys. Rev. A **44**, 7493 (1991).
12. H. Li and D. Wang, Chin. Opt. Lett. **9**, 030604 (2011).
13. J. M. Soto-Crespo, Ph. Grelu, and N. Akhmediev, Opt. Express **14**, 4013 (2006).
14. G. Wainblat and B. A. Malomed, Phys. D **238**, 1143 (2009).
15. A. W. Snyder, D. J. Mitchell, L. Polodian, and F. Ladouceur, Opt. Lett. **16**, 21 (1991).
16. A. W. Snyder and A. P. Sheppard, Opt. Lett. **18**, 482 (1993).
17. C. Pigier, R. Uzdin, T. Carmon, M. Segev, A. Nepomnyashchy, and Z. H. Musslimani, Opt. Lett. **26**, 1577 (2001).
18. G. I. Stegeman and M. Segev, Science **286**, 1518 (1999).
19. W. Królikowski and S. A. Holmstrom, Opt. Lett. **22**, 369 (1997).
20. E. A. Ultanir, G. I. Stegeman, C. H. Lange, and F. Lederer, Opt. Lett. **29**, 283 (2004).
21. A. Kamagate, Ph. Grelu, P. Tchofo-Dinda, J. M. Soto-Crespo, and N. Akhmediev, Phys. Rev. E **79**, 026609 (2009).
22. S. Gatz and J. Herrmann, IEEE J. Quantum Electron. **28**, 1732 (1992).
23. D. R. Neill, J. Atai, and B. A. Malomed, J. Opt. A **10**, 085105 (2008).
24. N. Akhmediev, J. M. Soto-Crespo, and Ph. Grelu, Chaos **17**, 037112 (2007).
25. L. Zheng and Y. Tang, Chin. Phys. B **19**, 044209 (2010).
26. C. Hang and G. Huang, Chin. Opt. Lett. **7**, 549 (2009).
27. K. Zhou, Z. Guo, and S. Liu, Chin. Opt. Lett. **8**, 791 (2010).